



## Validation and application of a membrane filtration evaluation protocol for oil-water separation

Mashaël Al-Maas<sup>a</sup>, Altaf Hussain<sup>a</sup>, Joel Minier Matar<sup>a</sup>, Deepalekshmi Ponnamma<sup>b</sup>,  
 Mohammad K. Hassan<sup>b</sup>, Mariam Al Ali Al-Maadeed<sup>b,c</sup>, Karim Alamgir<sup>d</sup>, Samer Adham<sup>a,b,\*</sup>

<sup>a</sup> ConocoPhillips Global Water Sustainability Center, Qatar Science & Technology Park, PO Box 24750, Doha, Qatar

<sup>b</sup> Center for Advanced Materials, Qatar University, PO Box 2713, Doha, Qatar

<sup>c</sup> Materials Science & Technology Program, College of Arts & Sciences, Qatar University, PO Box 2713, Doha, Qatar

<sup>d</sup> Department of Chemical & Biomolecular Engineering, University of Houston, Houston, Texas 77204, USA

### ARTICLE INFO

#### Keywords:

Ultrafiltration  
 Microfiltration  
 Oil-water separation  
 Membrane filtration  
 Experimental protocol

### ABSTRACT

Membrane filtration processes like microfiltration (MF) and ultrafiltration (UF) are proven to be effective in industrial wastewater treatment, including oil-water separation, as they generate suitable quality permeate for water reuse applications. Various research efforts have been conducted in areas of developing and/or modifying commercial MF/UF membrane materials through synthesizing new advanced polymers that promise improvement in oil-water separation performance. Although multiple MF/UF testing procedures were developed, there is still a gap in literature on having a comprehensive protocol that assesses the performance of the membranes in terms of flux, rejection, fouling, and cleanability. This paper delivers a robust bench scale testing procedure incorporating experiences and lessons learned from literature. The evaluation procedure includes three main testing steps: initial characterization, operating performance, and cleaning and recovery. The protocol was designed to mimic industrial conditions by using a representative synthetic produced water solution and operating multiple consecutive cycles of oil-water filtration followed by membrane chemical cleaning. The procedure was initially validated on multiple commercial MF/UF membranes having different pore sizes/MWCOs and chemistries obtained from various manufacturers and then applied to evaluate emerging membrane materials. The protocol was found to be reliable in evaluating the performance trends of various commercial membranes and effective in comparing the performance of emerging membranes. The developed procedure is proposed to be applied by researchers to assess the performance of new membrane materials as compared to relevant commercial products.

### 1. Introduction

Large volumes of oily wastewater are produced in various industrial processes such as oil and gas, refinery, petrochemical facilities, textiles, leather manufacturing and food processing [1–5]. For oil and gas industry, treatment of such oily wastewaters typically involves applying conventional oil removal technologies such as gravity separation, flotation, coagulation, and centrifugation, which are used to remove free and dispersed oil [6–8]. However, there have been recent drivers towards applying advanced treatment as the industry encounters new operational challenges related to strict environmental oil-in-water discharge limits and restrictions on deep well injection. As these water-reuse facilitating drivers are being recognized by the industry,

many oil and gas companies have started to investigate opportunities for applying fit-for-purpose treatment on by-product waters that are now considered a valuable resource instead of a possible liability. Membrane processes such as microfiltration (MF) and ultrafiltration (UF) are known to be one of the best available advanced treatment technologies that can generate suitable quality effluent for water reuse applications. These polymeric membranes offer lower energy consumption, high organics removal and compact systems with full automation. The main shortcoming is fouling due to adsorption of oil droplets onto the surface and internal pores which limits their performance and reduces their respective lifespan [8,9].

Polymeric flat/hollow-fiber MF/UF membranes used for the treatment of oily wastewater acquire different chemistries such as polyvinyl

\* Corresponding author at: Center for Advanced Materials, Qatar University, Doha, Qatar.

E-mail address: [sadham@qu.edu.qa](mailto:sadham@qu.edu.qa) (S. Adham).

<https://doi.org/10.1016/j.jwpe.2021.102185>

Received 15 February 2021; Received in revised form 2 June 2021; Accepted 12 June 2021

Available online 23 July 2021

2214-7144/© 2021 The Author(s). Published by Elsevier Ltd. This is an open access article under the CC BY license (<http://creativecommons.org/licenses/by/4.0/>).

acetate, polyacrylonitrile (PAN), polyvinylidene difluoride (PVDF), polysulfone, polyether sulfone (PES), cellulose acetate, etc. [10]. Various commercial polymeric MF and UF membranes tested on oily wastewater have shown high performances in terms of oil removal, fouling propensity, and cleanability. For instance, a tubular MF PAN membrane showed an oil removal efficiency of >99.7% and the membrane flux was restored by cleaning with citric acid and caustic anionic detergent [11]. Another hydrophilic UF PAN membrane at 20 kDa was investigated in bench scale for the treatment of a refinery oily wastewater. The membrane showed removals of 99% for oil and grease (O&G), total suspended solids (TSS) and turbidity [12].

Commercial UF membranes are typically prepared by phase inversion method in which the liquid polymer solution is converted to a solid state. The process involves mixing polymers, solvents, non-solvents, and even additives to form a solution that is casted on a surface for evaporation. The casted film is then immersed in a coagulation bath which leads to the separation of the solid membrane film [13]. The composition of the casting solution, the incorporation of additives, and the alteration in the casting temperature, thickness and evaporation time are examples of parameters that can be optimized to enhance the membrane's characteristic properties and performance [14]. The pore characteristics and skin layer morphology are improved in the casting step to obtain required molecular weight cut-off (MWCO). The MWCO term was derived from the rejection of macromolecules described by their molecular weights. Arbitrarily, the MWCO can be defined as the rejection of 90% of a known molecular weight organic solute [15,16]. Hence, UF membranes do not possess an absolute pore size and the fabrication of such membranes has been an elusive target for many years. To date, there is not a standard method followed by membrane manufacturers for characterizing the MWCO. Yet, membrane manufacturers often use dextran, polyethylene glycol (PEG) and polyvinylpyrrolidone (PVP) as solutes for determining the membrane MWCO [16,17]. On the other hand, numerous research efforts have been conducted towards modifying commercial products or developing novel alternatives that potentially show a step change in performance. Improvement of commercial products involves surface modification via addition of nanoparticles namely alumina, bentonite, silica, titanium oxide and zinc oxide to increase the hydrophilicity and antifouling behavior of the membrane [18–23]. Most recently, fabrication of flat sheet UF membranes consisting of self-assembled block copolymer (BCP) films has gained wide popularity since they possess enhanced water fluxes [17,18,24–30].

With all emerging MF/UF membranes specifically flat sheet type being developed, there is a pressing need for having a representative bench scale testing protocol for evaluating and comparing the performance of newly developed membranes against commercial products. After extensively reviewing various bench scale testing procedures applied in literature [17,20,25,26,29,31–37], it was observed that these published testing protocols were developed targeting the evaluation of a specific performance parameter. This has created a gap in terms of having one comprehensive testing procedure addressing all basic membrane performance parameters like permeability, rejection, fouling tendency, and recyclability. Another key aspect of the testing protocol is the feed solution. Since access to actual industrial oily wastewaters (e.g. produced water (PW)) is restricted due to the associated health, safety, and environmental (HSE) challenges, the use of synthetic recipes in performance screening tests has become more applicable [38–44].

## 2. Objective

Based on the above, research experience and lessons learned from literature were considered to develop a robust bench scale testing procedure that assesses the performance of flat sheet MF/UF membranes for industrial applications in terms of water permeability, organics rejection, fouling tendency, and cleanability. The developed procedure was initially validated on several commercial membranes via examining the

effect of varying pore size/MWCO, manufacturer, and chemistry on the oil-water separation performance. The protocol was then applied on selected emerging membranes for performance comparison to commercial products.

## 3. Materials & methods

### 3.1. Chemicals

- **Deionized water (DI):** resistivity of  $\approx 18 \text{ M}\Omega\text{-cm}$  provided by Milli-Q ultrapure water system (integral, 10, Millipore).
- **Salts:** sodium chloride, calcium chloride dihydrate, magnesium chloride hexahydrate, potassium chloride, sodium sulfate, ammonium chloride, sodium bicarbonate all at 99% purity from Sigma Aldrich.
- **Oil:** Crude oil from operation:  $^{\circ}\text{API}$ : 38.7, density (g/ml) @ 25  $^{\circ}\text{C}$ : 0.825.
- **Emulsifier:** Sodium dodecyl sulfate (SDS) obtained from Thermo Fischer Scientific.
- **Reagent:** Sodium hydroxide pellets - NaOH acquired from Thermo Fischer Scientific.

### 3.2. Synthetic PW solution preparation

Oil-water separation tests were carried out using a representative synthetic PW solution prepared following the protocol published by [45]. The recipe involves using: a low salinity brine (total dissolved solids (TDS):  $\sim 3800 \text{ mg/L}$ ) mimicking the salinity of a gas field PW [46], a medium grade neat crude oil and an emulsifier (SDS) to disperse the oil into the brine in a ratio of 5:1 (oil to surfactant). Since MF/UF membrane treatment is typically applied for tertiary industrial wastewater treatment, a solution having a total organic carbon (TOC) concentration in the range of 25–30 mg/L was prepared. Initially, 500 mL of low salinity brine was prepared using DI water and salt concentrations specified in Table 1. Then,  $\sim 5 \text{ mg}$  of SDS were added to the brine with 0.03 mL of crude oil. The solution was then magnetically stirred at 1000 rpm for 0.5 h and sonicated for another 0.5 h. Finally, the solution was transferred to a glass separatory funnel to settle for 1–2 h. After separating the free oil layer, the final solution was stored in a glass bottle and used immediately in the oil-water separation tests. A summary of the analytical results for the synthetic PW solution are presented in Table 2. Fig. 1 presents the particle size distribution of the final solution showing a mean droplet size of 4.6  $\mu\text{m}$  which is within the typical size range of oil-water emulsions at  $< 20 \mu\text{m}$  [47].

**Table 1**  
Concentration of salts used to prepare the low salinity brine.

Salt	Concentration (g/L)
NaCl	2.39
CaCl <sub>2</sub> ·2H <sub>2</sub> O	1.10
MgCl <sub>2</sub> ·6H <sub>2</sub> O	0.52
KCl	0.10
Na <sub>2</sub> SO <sub>4</sub>	0.07
NH <sub>4</sub> Cl	0.03
NaHCO <sub>3</sub>	0.14

**Table 2**  
Analytical characteristics for the synthetic PW.

Parameter	Synthetic PW
pH	7.8
Conductivity (ms/cm)	7.2
TOC (mg/L)	25–30
O&G (mg/L)	26–32

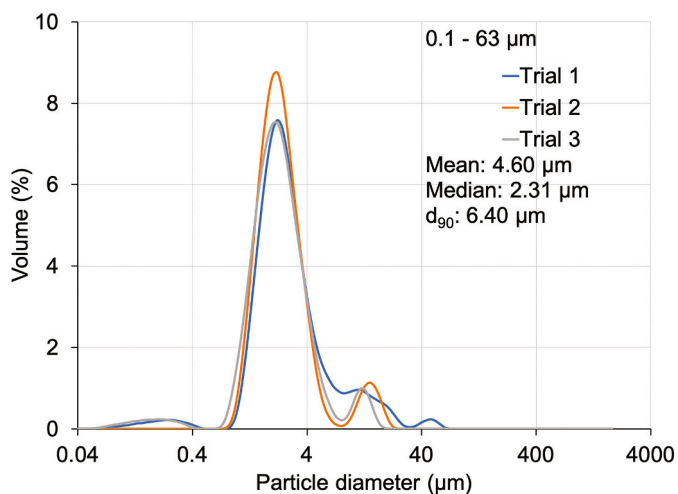


Fig. 1. Particle size distribution of the synthetic PW [45].

**Table 3**  
Summary of analytical characterization equipment.

Analysis	Instrument model
TOC	TOC-V, Shimadzu
O&G	TD560 by Turner Designs Hydrocarbon Instruments
Scanning electron microscope (SEM)	Nova NanoSEM 450
Optical contract angle	OCA, Datapysics
Fourier-transform infrared (FTIR) spectroscopy	Nicolet 6700 FT-IR spectrometer
Particle size distribution	Beckman and Coulter Analyzer, Model LS 13320

### 3.3. Analytical & characterization methods

#### 3.3.1. Analytical equipment (Table 3)

#### 3.3.2. Thickness, porosity, and mean pore radius

The porosity ( $\epsilon$ ) of the membrane was measured following a protocol published by [48]. The gravimetric method determines the porosity of a membrane based on the difference between the wet and dry weights ( $w_1$  and  $w_2$ ) of a known membrane area  $A$  and thickness  $L$  as indicated in Eq. (1).

$$\epsilon = \frac{w_2 - w_1}{A \times L \times D_w} \quad (1)$$

where  $D_w$  is the water density of  $0.998 \text{ g/cm}^3$ . To measure porosity, initially a piece of known membrane area was soaked for 24 h in DI water. Then, the sample was weighed immediately after cautiously cleaning excess water on the membrane surface. After that, the membrane sample was dried in the oven for 2 h at a temperature of  $60 \text{ }^\circ\text{C}$  and then weighed again. The thickness of the membrane was measured directly using a Pocket Thickness Gauge  $0."/0.001"$  micrometer. The mean pore radius ( $R_m$ ) was then calculated using Eq. (2):

$$R_m = \sqrt{\frac{(2.9 - 1.75\epsilon) \times 8\eta L J_w}{A \times \epsilon \times \Delta P}} \quad (2)$$

where  $\eta$  is the viscosity of water at  $8.9 \times 10^{-4} \text{ Pa s}$ ,  $J_w$  is the membrane water flux in  $\text{m}^3/\text{s}$ , and  $\Delta P$  is the applied operating pressure in (Pa). Analyses were carried out on triplicate membrane samples to ensure results repeatability.

#### 3.4. MF/UF bench scale setup

The bench scale unit was built after reviewing published MF/UF testing setups [14,24,25,27]. As shown in Figs. 2 and 3, the setup is

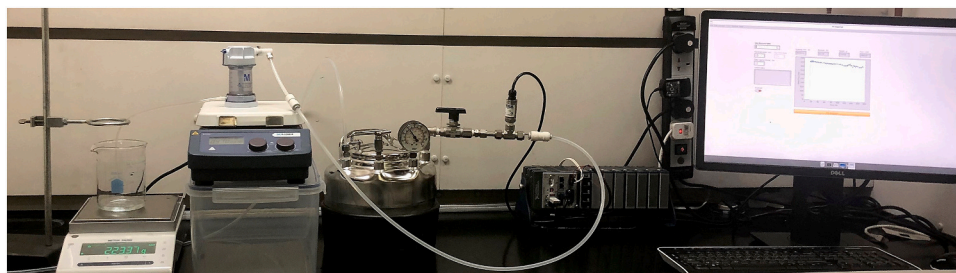


Fig. 2. MF/UF bench scale setup.

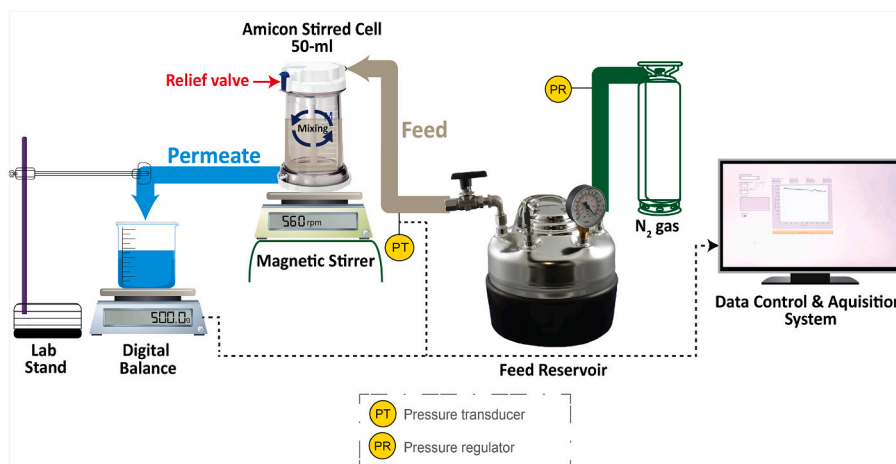


Fig. 3. MF/UF bench scale diagram.

based on an Amicon UF stirred cell (Amicon, Millipore, USA) having a capacity of 50 mL, membrane diameter of 44.5 mm, and an actual filtration area of 13.5 cm<sup>2</sup>. The cell is used for testing flat sheet membranes at different pressures ranging from 1 to 5 bar. Those pressures were provided using a nitrogen cylinder connected to a 1-gallon feed reservoir (316SS pressure vessel, Sterlitech, USA) with appropriate safety features (pressure regulator and relief valve). A pressure transducer (PX309, Omega Engineering, USA) was mounted at the inlet of the Amicon UF stirred cell (i.e. feed reservoir outlet) to accurately measure and record the applied pressure. The Amicon UF stirred cell was positioned on top of a magnetic stirring plate (Sterlitech, USA) to maintain the homogeneity of the feed wastewater. Filtered water (i.e. permeate) was collected in a 1 L glass beaker that was placed on a digital balance (Mettler Toledo, Switzerland) to measure the weight of the collected water. Both pressure and permeate weight were acquired every 250 ms by a LabVIEW acquisition system (cRIO-9035, National Instruments, USA). The system was setup to constantly collect and store the data as well as to monitor the membrane water flux that is plotted by the software and displayed on a screen.

### 3.5. Commercial MF/UF membranes

Several commercially available MF/UF membranes from various manufacturers with different chemistries and MWCOs were screened, and some were selected for testing using the developed experimental protocol as shown in Table 4.

### 3.6. MF/UF experimental protocol

After thoroughly reviewing published MF/UF bench-testing experiences and not coming across a comprehensive procedure, a testing protocol was developed addressing membrane permeability, rejection, fouling and cleanability which consists of three key steps:

#### 3.6.1. Initial characterization

The membrane sheet was initially soaked in DI water for at least 24 h to ensure that any shipping or storage preservatives have been washed out properly. After that, the membrane was cut and placed into the Amicon UF stirred cell used for testing (diameter: 44.5 cm). The membrane was then tested using DI water at a pressure of 3 bar and stirring speed of 560 rpm until reaching a stable water flux measurement. Similar operating conditions were also applied for all following baseline tests. Flux obtained from this test is referred to as the “clean membrane flux” which was utilized as the benchmark for flux comparison against the fouled membrane.

#### 3.6.2. Operating performance

Fouling tests were performed using a low salinity synthetic PW solution as noted in Section 3.2. Targeting 50% feed volume reduction, 100 mL and 50 mL of the synthetic PW were transferred to the 1-gal feed reservoir and the Amicon UF stirred cell, respectively. The membrane

**Table 4**  
Selected commercial MF and UF membranes.

Manufacturer	Category	Chemistry	Size µm	MWCO kDa
M1	MF	PES	8.0	n.a.
M1	MF	PES	0.2	n.a.
M2	UF	PES	n.a.	300
M2	UF	PES	n.a.	100
M2	UF	PES	n.a.	50
M2	UF	PVDF	n.a.	100
M2	UF	PAN	n.a.	100
M3	UF	PAN	n.a.	50
M4	UF	PAN	n.a.	20

n.a.: Not applicable.

was then tested at a pressure of 3 bar and stirring speed of 560 rpm. The flux generated from this test is described as the “synthetic PW flux”. Samples of feed and permeate were collected and analyzed for TOC and O&G to assess the organics rejection performance by the membrane.

#### 3.6.3. Cleaning and recovery

Initially, the “fouled membrane flux” was measured via performing a DI water baseline on the fouled membrane. After that, two membrane chemical cleaning steps were implemented to recover the membrane's lost flux due to fouling. For the first step, 50 mL of a ~1 mM NaOH solution with pH of ~11.5 at a temperature of ~25 °C was prepared and transferred to the Amicon UF stirred cell for surface cleaning under magnetic stirring for 15 min at 560 rpm. To measure the efficiency of NaOH cleaning, a DI water baseline test was performed as noted in Section 3.6.1. The second chemical cleaning step involves using 50 mL SDS solution at a concentration of ~10 mM, a pH of ~9.4 and a temperature of 35 °C at similar testing conditions followed for NaOH cleaning. A final baseline test was conducted for measuring the final membrane flux “chemical cleaning flux” and determining the total flux loss due to fouling as indicated in Eq. (3).

$$\text{Flux loss} = \frac{J_0 - J_f}{J_0} \times 100\% \quad (3)$$

where  $J_0$  is the “clean membrane” flux and  $J_f$  is the final membrane flux after “chemical cleaning”.

To mimic typical membrane filtration operating conditions, after characterizing the clean membrane water flux (step 3.6.1), three consecutive cycles of membrane fouling and cleaning were conducted as a robust approach for determining the membrane's oil-water separation efficiency.

## 4. Results & discussion

### 4.1. Protocol validation on commercial MF/UF membranes

Validation tests using the developed bench-scale testing procedure were carried out on selected commercial MF and UF membranes as specified in Table 4. The applicability of the testing protocol was evaluated for different membrane parameters including variation of membrane pore size/MWCO, manufacturer, and chemistry.

#### 4.1.1. Variation of pore size/MWCO

**4.1.1.1. MF membranes.** The impact of pore size was first studied on commercial MF membranes. 0.2 and 8.0 µm PES membranes were obtained from M1 and tested using the developed protocol. Since higher water fluxes are expected from MF membranes in comparison to UF, the operating pressure was adjusted and set at 0.5 bar. Such adjustment will prolong the testing period which ultimately will help in better characterizing the performance of the membrane. Fig. 4 compares the oil-water separation test results for both membranes. Specific water fluxes of 10,689 and 28,616 LMH/bar were observed for the 0.2 and 8.0 µm PES membranes, respectively. In terms of organics rejection, an average TOC rejection of 87% was obtained for the 0.2 µm membrane against 67% for the 8.0 µm membrane as noted in Table 5. The lower TOC rejection obtained at a pore size of 8.0 µm is attributed to the synthetic PW solution that consists of oil-water emulsions possessing a mean droplet size of 4.6 µm. Therefore, the 8.0 µm membrane is not rejecting smaller oil particles which results in lower TOC rejection. Similar interpretation applies also for the minimum flux loss obtained at this pore size against the 26% loss for the 0.2 µm PES membrane that is rejecting the smaller oil contaminants.

#### 4.1.1.2. UF membranes.



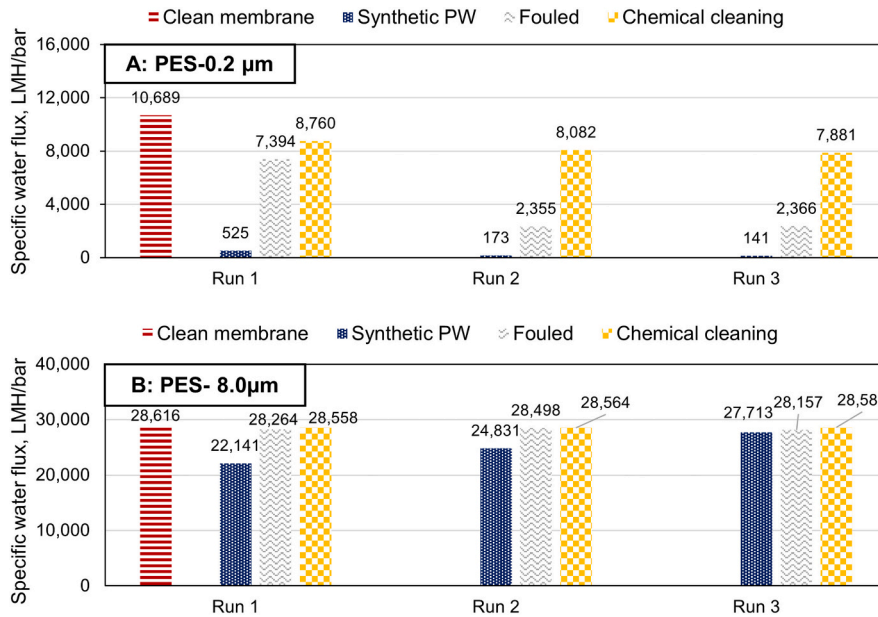


Fig. 4. MF test results for M1-PES, A: 0.2 μm and B: 8.0 μm.

Table 5

MF membranes - organics rejection results.

Membrane	TOC rejection <sup>a</sup> %
M1-PES-0.2	87% ± 2%
M1-PES-8.0	67% ± 1%

<sup>a</sup> Average TOC rejection for three consecutive filtration cycles.

A. Oil-water separation tests

As UF membrane manufacturers use different methods for MWCO characterization, three commercial UF membranes with PES chemistry having different MWCOs of 50, 100, and 300 kDa were acquired from manufacturer M2 and tested using the developed protocol. As shown in Fig. 5, specific water fluxes of 21, 41, and 59 LMH/bar were obtained for the tested MWCOs (50–100–300 kDa), respectively. The variation in flux

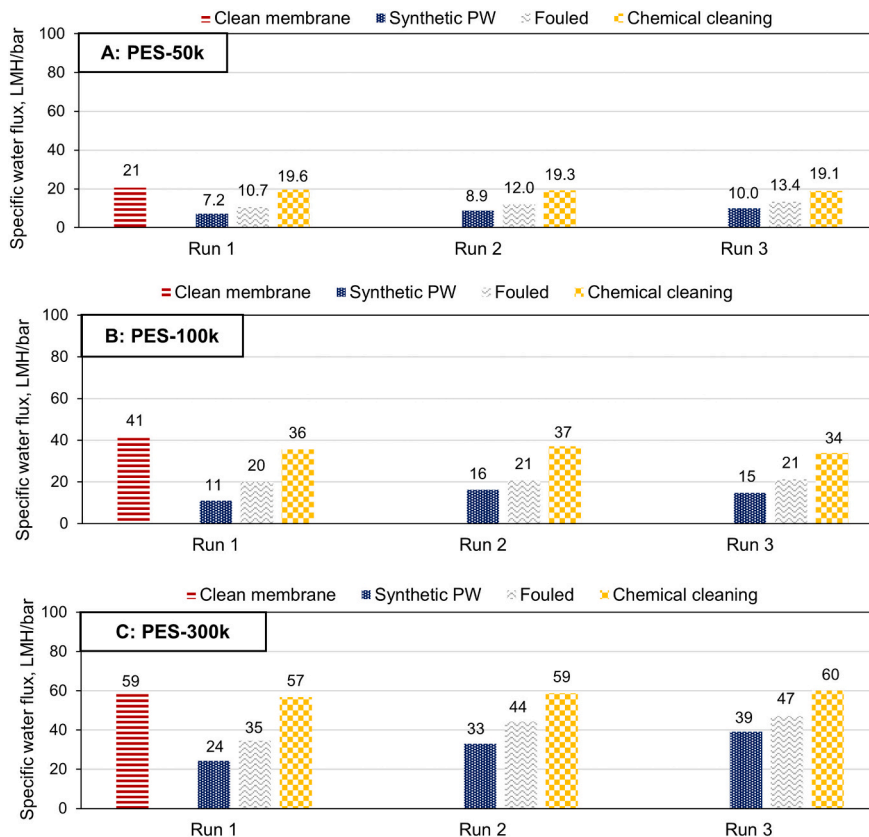


Fig. 5. UF test results for M2-PES membranes, A:50, B:100, and C:300 kDa.

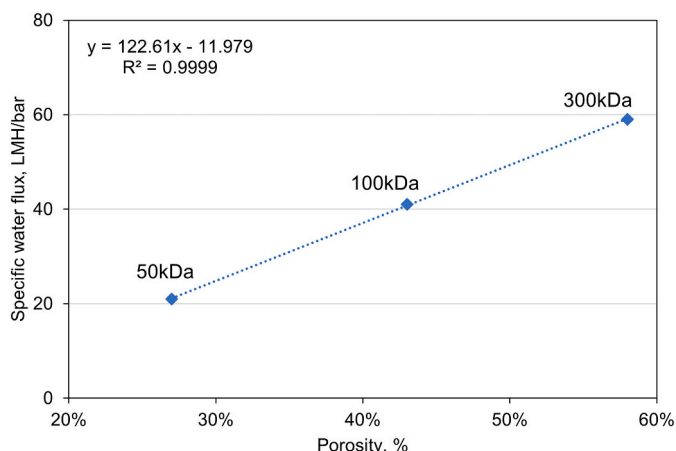


Fig. 6. Correlation between specific water flux and porosity for different MWCOs.

against MWCO obtained using the protocol was validated with porosity measurements as presented in Fig. 6. Both sets of data were found to show a strong linear correlation validating the applicability of the procedure in characterizing the pure water permeability of membranes having different MWCOs. In Table 6, O&G analyses performed on feed and permeate samples showed comparable rejection performances for all MWCOs with >99% removal. In terms of TOC, as expected, lower removal performances were realized in comparison to O&G at ~88% for 100 k and 300 k against ~92% for 50 k. This is due to the physical breaking of the oil-SDS emulsions by the membrane that is mainly rejecting the oil and allowing the SDS molecules to permeate inside the membrane pores thus contributing to the TOC in the permeate as shown in Table 6. PES-50 kDa was selected as an example to graphically represent the oil emulsions breaking mechanism through the tested membranes as illustrated in Fig. 7 [49].

Table 6  
Fouling and organics rejection results for PES-50, 100, and 300 kDa from M2.

Membrane	Flux loss %	TOC rejection <sup>a</sup> %	O&G rejection <sup>a</sup> %	Permeate TOC <sup>a</sup> mg/L	Permeate O&G <sup>a</sup> mg/L
M2-PES-50 k	8%	92% ± 1%	99.3% ± 0.1%	2.0 ± 0.3	0.2 ± 0.0
M2-PES-100 k	18%	88% ± 1%	99.2% ± 0.4%	3.3 ± 0.2	0.3 ± 0.0
M2-PES-300 k	0%	88% ± 1%	99.4% ± 0.1%	3.1 ± 0.2	0.2 ± 0.0

<sup>a</sup> Average rejection of three consecutive oil-water separation cycles.

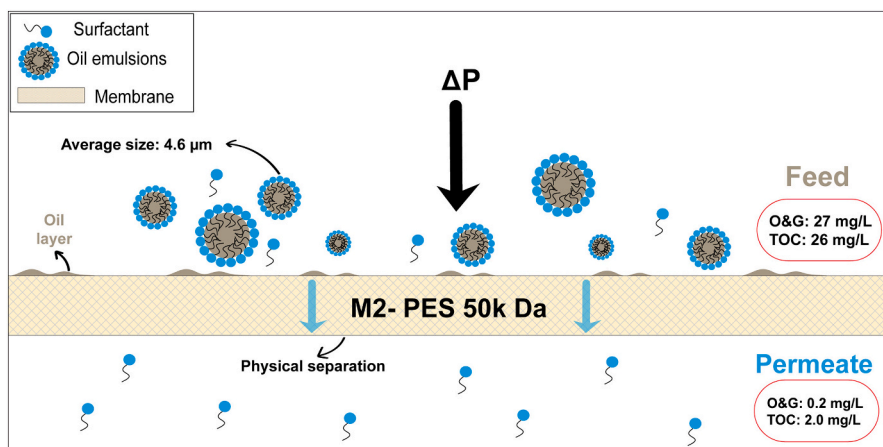


Fig. 7. Graphical representation of the oil emulsions breaking mechanism for M2-PES-50kDa membrane.

Table 7  
Membrane fouling correlations [50,51].

Fouling mechanism	Flux equation	Linear expression	Schematic
Cake filtration (surface deposition)	$J = \frac{J_o}{(1 + J_o^2 kt)^2}$	$\frac{1}{J^2} = \frac{1}{J_o^2} + kt$	
Intermediate blocking	$J = \frac{J_o}{1 + J_o kt}$	$\frac{1}{J} = \frac{1}{J_o} + kt$	
Standard blocking	$J = \frac{J_o}{(1 + J_o^2/2 kt)^2}$	$\frac{1}{\sqrt{J}} = \frac{1}{\sqrt{J_o}} + kt$	
Complete blocking	$J = J_o \exp(-kt)$	$\ln\left(\frac{1}{J}\right) = \ln\left(\frac{1}{J_o}\right) + kt$	

Where J is the water flux, J<sub>o</sub> is the initial water flux, t is filtration time and k is a kinetic parameter.

### B. Modeling of fouling mechanisms

The protocol was also utilized to compare the membranes' fouling propensity in terms of total irreversible flux loss. Four classic fouling correlations [50,51] were curve-fitted to the experimental data to identify the fouling mechanism occurring on the membrane. As indicated in Table 7, in the cake filtration mechanism, the layers of contaminants deposit on the membrane surface, whereas in complete blocking, foulants will entirely block the pores of the membrane. Similarly, in intermediate blocking the contaminants will block some of the pores on the membrane with some attaching to formerly deposited particles. The last fouling mechanism is the standard blocking of the pores at which the size of the contaminant particles is smaller than the membrane pores causing them attach to the inner walls of the pores.

Results presented in Table 6 showed an increase in total flux loss to

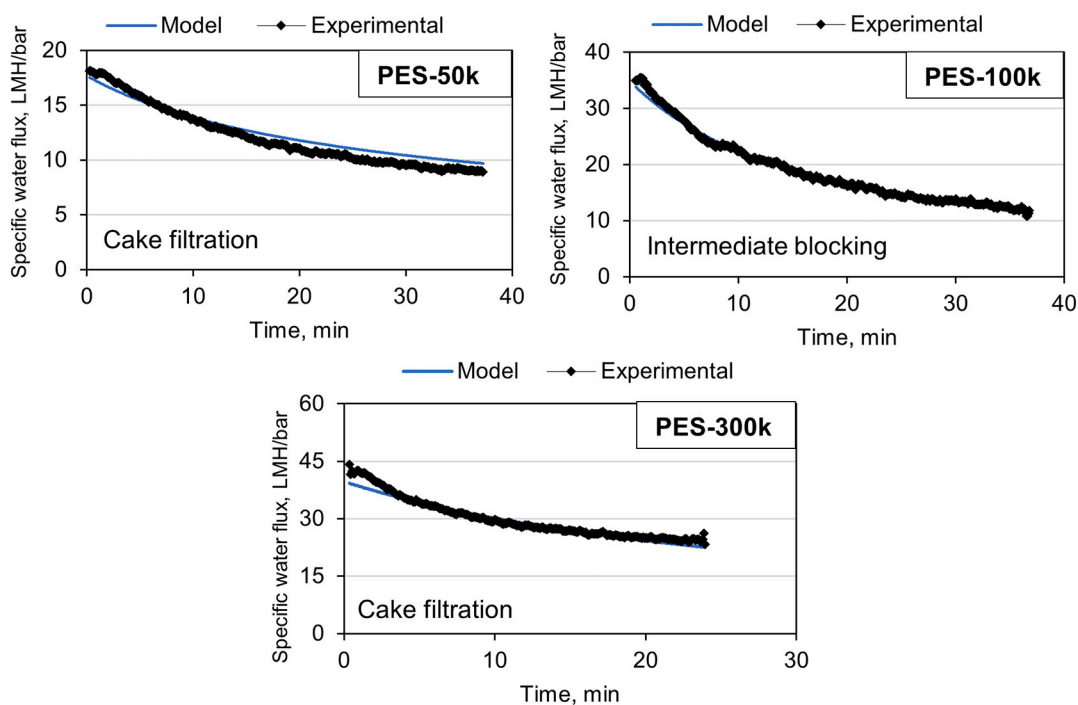
**Table 8**  
Correlation coefficient ( $R^2$ ) for tested MWCOs.

Membrane	MWCO, kDa	Cake filtration	Intermediate blocking	Standard blocking	Complete blocking
		$R^2$			
M2 – PES	50	0.99	0.97	0.95	0.92
	100	0.87	0.97	0.96	0.95
	300	0.97	0.95	0.93	0.91

about 18% at a MWCO of 100 kDa against 8% obtained at 50 kDa. Nevertheless, at a higher MWCO of 300 kDa irreversible fouling behavior was detected to be minimum (i.e. 0% flux loss). The fouling behavior for those membranes was studied further through applying the classic fouling correlations. Table 8 compares the correlation coefficients ( $R^2$ ) for the four fouling mechanisms. At a MWCO of 50 kDa, surface deposition (cake filtration) was found to have the highest  $R^2$  of

0.99 which showed the best agreement with experimental data as shown in Fig. 8, confirming that surface deposition was the main fouling mechanism for this membrane.

Similar approach was applied for MWCOs of 100 and 300 kDa. Results showed that at a MWCO of 100 kDa, intermediate blocking generated the best fit at an  $R^2$  coefficient of  $\sim 0.97$ . This justifies the experimentally obtained increase in total flux loss at this MWCO in comparison with the 50 kDa membrane since at intermediate fouling some of the foulants will deposit while others will block the surface pores of the membrane. At a higher MWCO (300 kDa), cake filtration was found to be the main fouling mechanism at an  $R^2$  of 0.97, and with the larger pore size on this membrane the applied surface cleaning will potentially be more efficient as it can reach through the larger pores and remove deposited or blocking contaminants from the membrane.

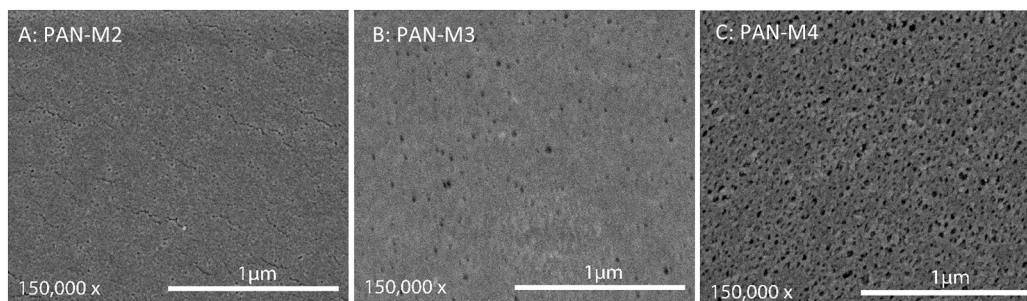


**Fig. 8.** Best-fit fouling correlations against experimental data for PES-M2 membranes at 50 kDa (top left), 100 kDa (top right), and 300 kDa (bottom).

**Table 9**  
Summary of UF test results for PAN membranes-M2, M3, and M4.




Polymer	Vendor/MWCO kDa	Specific flux (LMH/bar)	Flux loss %	*TOC rejection %
PAN	M2-100	16	0%	80% ± 1%
	M3-50	203	51%	86% ± 1%
	M4-20	390	7%	80% ± 1%

\* Average rejection of three consecutive oil-water separation cycles



**Fig. 9.** SEM images for A: PAN-M2 (right), B: PAN-M3 (middle), and C: PAN-M4 (left).

**Table 10**  
Contact angle results for PAN, PES, and PVDF.

Membrane chemistry	Water contact angle (°)		
	This work	Image (after 1 s)	Published data
PAN	56° ± 1°		57 [19]
PES	50° ± 2°		52 [52]
PVDF	69° ± 1°		74 [53]

4.1.2. Variation of vendor

As properties and performance of a membrane are both dependent on the synthesis method and thus its manufacturer. Hence, the developed protocol was also applied for evaluating the effect of varying membrane vendor using three PAN membranes obtained from M2, M3, and M4 with MWCOs of 100, 50 and 20 kDa, respectively. Table 9 summarizes the testing results in terms of flux, fouling, and rejection. Fluxes of

16, 203, and 390 LMH/bar were obtained for the tested PAN membranes. Despite that PAN sourced from M2 was characterized to have a MWCO of 100 kDa, it showed lower flux in comparison to PAN membranes sourced from M3 and M4 having MWCOs of 50 and 20 kDa. SEM images of the tested membranes are shown in Fig. 9. The figure compares the surface structure of the tested PAN membranes confirming that PAN-M4 has larger pores in comparison to PAN-M2. PAN-M3 was also showing relatively larger pores against PAN-M2, but they were less in terms of quantity against PAN-M4. In addition, the three membranes have shown different fouling performances. For instance, PAN-M2 and PAN-M4 revealed minimum fouling behaviors at total flux losses <10%, whereas PAN-M3 showed a higher flux loss at 51%. Similarly, both PAN membranes from M2 and M4 showed similar rejection performances at a TOC removal of 80%, while PAN from M3 showed a slightly higher TOC rejection at 86%. The above results prove the applicability of the testing protocol in assessing and comparing the performance of products sourced from different manufacturers.

4.1.3. Variation of chemistry

Three different membrane chemistries PES, PAN, and PVDF having a MWCO of 100 kDa were sourced from the same manufacturer (M2) to ensure having a common comparison basis for performance evaluation and were tested using the developed experimental procedure.

A. Water contact angle

Water contact angle analysis assessing the hydrophilicity of the three

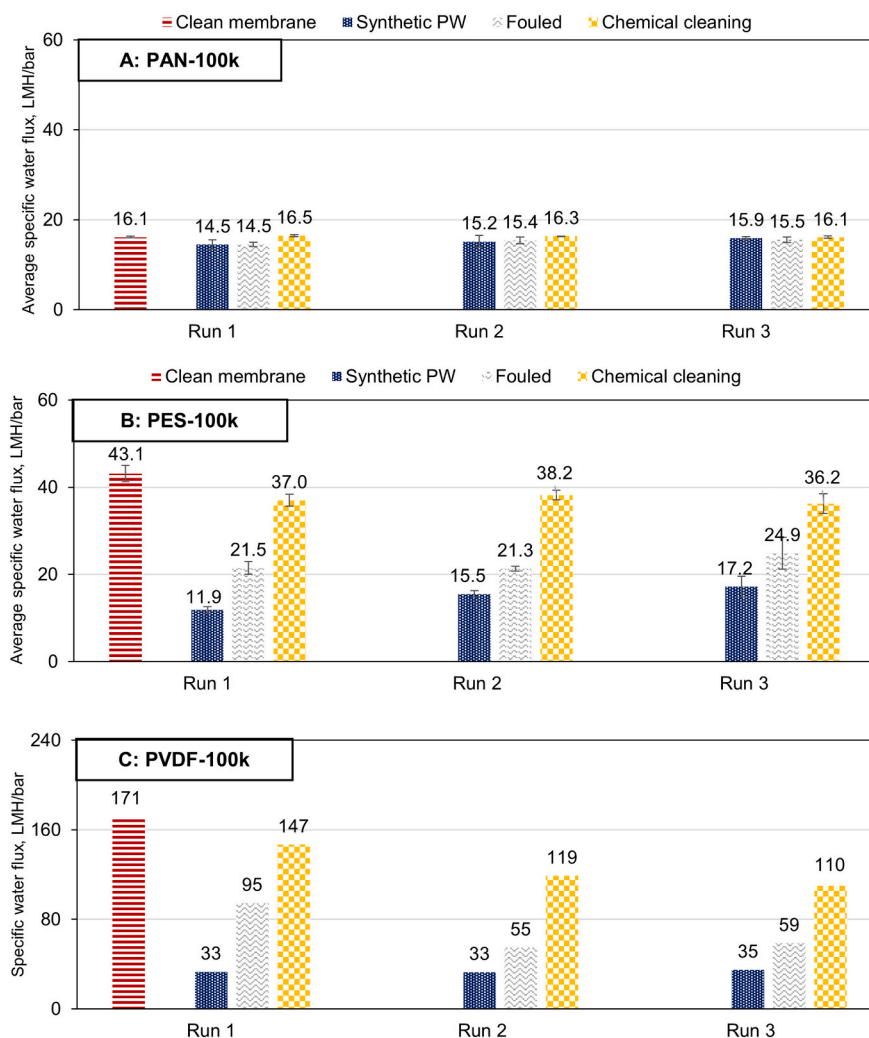


Fig. 10. Average UF test results on duplicate coupons for, A: M2-PAN-100 k and B: M2-PES-100 k. C: UF test results for M2-PVDF-100 k.



**Table 11**  
Reproducibility validation test - organics rejection results.

Membrane	Coupon #	TOC rejection <sup>a</sup> %
M2-PAN-100k	1	81% ± 2%
	2	80% ± 1%
M2-PES-100k	1	88% ± 1%
	2	87% ± 2%

<sup>a</sup> Average TOC rejection for three consecutive filtration cycles.

**Table 12**  
Oil-water separation test results for PAN, PES, and PVDF from M2 at 100 kDa.

Polymer	Flux loss %	TOC rejection <sup>a</sup> %	O&G rejection <sup>a</sup> %	$\epsilon$ %	R <sub>m</sub> nm
PAN	0%	80% ± 1%	99.5% ± 0.2%	38% ± 1%	35 ± 1
PES	18%	88% ± 1%	99.2% ± 0.4%	43% ± 1%	52 ± 1
PVDF	36%	93% ± 1%	99.4% ± 0.3%	57% ± 2%	92 ± 2

<sup>a</sup> Average rejection of three consecutive oil-water separation cycles.

**Table 13**  
Permeate TOC and O&G results for PAN, PES, and PVDF from M2 at 100 kDa.

Polymer	Permeate TOC <sup>a</sup> mg/L	Permeate O&G <sup>a</sup> mg/L
PAN	4.9 ± 0.1	0.2 ± 0.0
PES	3.3 ± 0.2	0.3 ± 0.0
PVDF	1.8 ± 0.2	0.3 ± 0.0

<sup>a</sup> Average rejection of three consecutive oil-water separation cycles.

membrane chemistries was carried out as shown in Table 10. Membranes having PAN and PES chemistries showed higher affinities towards water at contact angles between 50 and 56°. On the other hand, PVDF was found to be less hydrophilic at a measured water contact angle of 69° making it more susceptible to organic fouling. Obtained results were validated against published data and were all found to be equivalent [16].

## B. Oil-water separation tests

Initially, the reproducibility of the developed testing protocol in terms of showing repeatable performance results upon testing duplicate membrane coupons was validated. Duplicate membrane coupons for PAN and PES were tested and the average specific water flux results are presented respectively in Fig. 10A and Fig. 10B. Test results were found

to be reliably reproducible in terms of characterizing the membrane's pure water flux as well as the fouling behavior and organics rejection for both membrane chemistries as presented in Table 11.

Fig. 10 compares the performance of three different membrane polymers PAN, PES, and PVDF. Specific water fluxes of 16, 43, and 171 LMH/bar were obtained for the tested membranes, respectively. Although PES and PAN were proven to be more hydrophilic, both were showing lower membrane specific water fluxes against PVDF. Such performance was investigated through measurements of porosity and mean pore radius. Results were found to confirm such variation in flux between tested polymers with PVDF showing the highest porosity and mean pore size at 57% and 92 nm as presented in Table 12. The three membrane polymers were capable of removing almost all the O&G from the synthetic PW at percentages >99%, however in terms of TOC – attributed to both oil and SDS – both PES and PVDF chemistries have shown better TOC rejections against PAN. This was supported by permeate TOC and O&G data confirming the physical breakage of emulsions and the passage of SDS through the membranes as presented in Table 13 and illustrated in Fig. 7.

## C. FTIR analysis

To compare the fouling behavior of the three tested chemistries, FTIR analysis was carried out to identify key functional groups present in the crude oil used to prepare the synthetic PW and both the clean and the fouled membrane samples. Fig. 11 presents the FTIR absorbance spectra for the crude oil against the fouled membranes after subtracting the absorbance of the clean membranes. As shown in the figure, peaks found at wavelengths of 2292 and 2852 cm<sup>-1</sup> in the crude oil relate to single C–H stretching vibrations [54]. Similar peaks were also found on the three fouled membrane chemistries. FTIR results were found to agree with the experimentally obtained fouling trends in terms of verifying that PAN has the least fouling tendency against PES and PVDF.

## 4.2. Protocol application on emerging membranes

Based on the above validation study performed on commercial MF/UF products, we are in the process of applying and optimizing the protocol to a wide range of emerging membrane materials under development in order to effectively evaluate their performance for oil-water separation. Below are two examples for the application of the testing procedure on innovative membrane materials currently being developed.

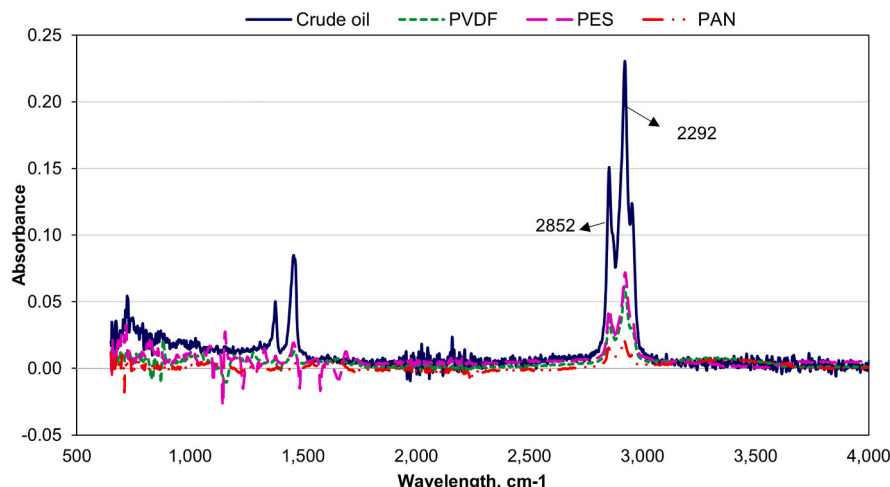


**Fig. 11.** Clean membrane subtracted FTIR spectra for crude oil (blue), PAN (red) and PVDF (green) and PES (pink).

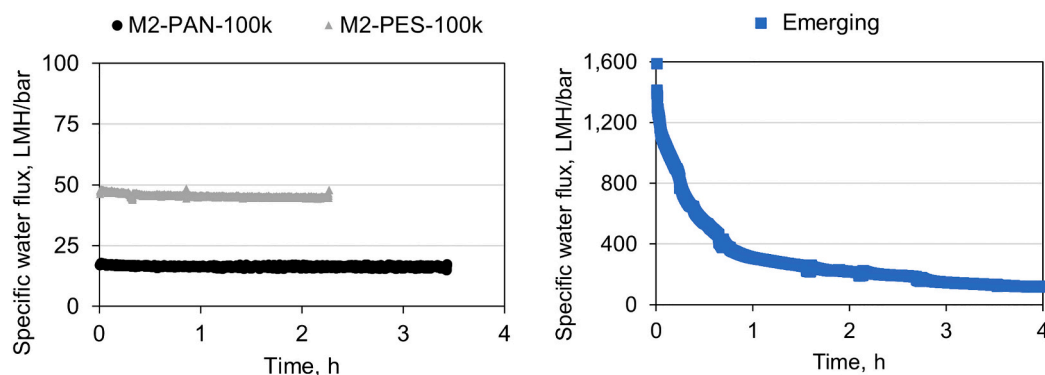


Fig. 12. Initial characterization test results for commercial (Left) and emerging (Right) membranes.

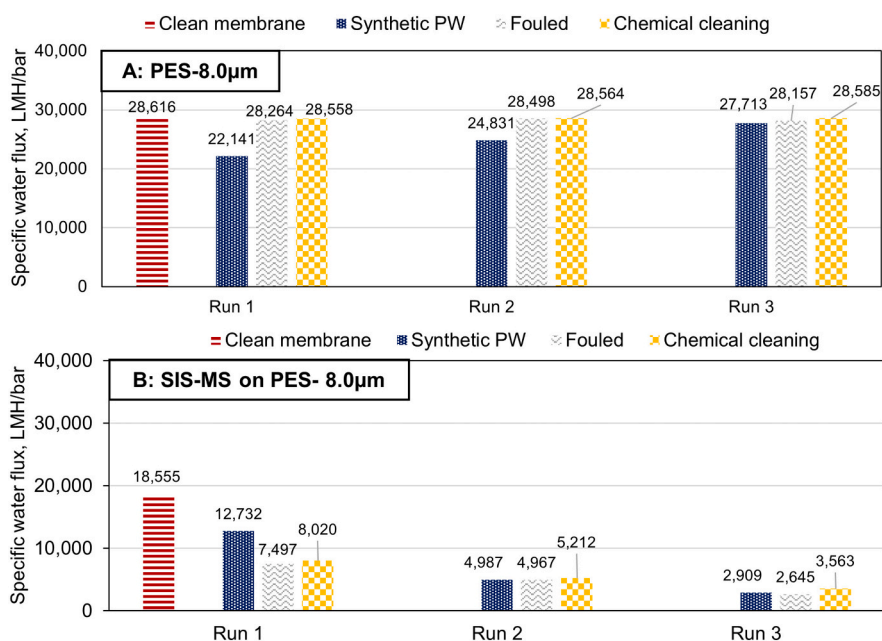


Fig. 13. UF test results for A: commercial PES-8.0 μm and B: emerging SIS-MS on PES-8.0 μm membrane.

4.2.1. Initial characterization

The first step of membrane testing as denoted in Section 3.6.1 is the membrane initial characterization that is performed using DI water. This critical test is performed on a clean membrane sheet to determine its stable pure water permeability prior to fouling tests. Fig. 12 compares the water flux results for two commercial membranes: PAN-100 k, PES-100 k manufactured by M2 against an emerging membrane under development. As expected, both commercial membranes were consistently showing stable water flux measurements after only the first half hour of testing. On the other hand, one of our emerging UF membranes under development showed significant drop in flux up to ~91% during the first 3 h before starting to stabilize during the last hour of testing. Such challenge related to the initial membrane characterization was identified as an area that needs further optimization by the emerging membrane developers.

4.2.2. Oil-water separation test

An experimental nanostructure enhanced MF membrane developed by our team was also tested using the developed protocol. The membrane consists of a styrene-isoprene-styrene (SIS) block copolymer/mesoporous silica (MS) nanocomposite layered on a commercial 8.0 μm PES MF membrane sourced from M1. The specific water flux measured for the modified membrane was found to be lower at ~18,600 LMH/bar

Table 14

Emerging membranes - organics rejection results.

Membrane	TOC rejection <sup>a</sup> %
PES-8.0 μm	67% ± 1%
SIS-MS-PES-8.0 μm	81% ± 2%

<sup>a</sup> Average TOC rejection for three consecutive filtration cycles.

in comparison to the commercial MF membrane being initially at ~28,600 LMH/bar. After testing it with the synthetic PW solution, a following baseline test confirmed the fouling of the emerging membrane at a specific water flux of ~7500 LMH/bar as shown in Fig. 13. Upon applying chemical cleaning, it was found that only a small fraction of the flux was recovered (i.e. <10%) in cycle 1. Similarly, cycles 2 and 3 confirmed the membrane's fouling tendency with a consistent drop in the "fouled" membrane flux as well as the insignificant flux recovery after chemical cleaning translating to a total flux loss of 81%. In terms of organics rejection, the nanocomposite coating was able to enhance the rejection of the 8.0 μm PES commercial membrane from 67% up to an average of 81% as demonstrated in Table 14. Thus, through applying the developed protocol, it was verified that this membrane showed

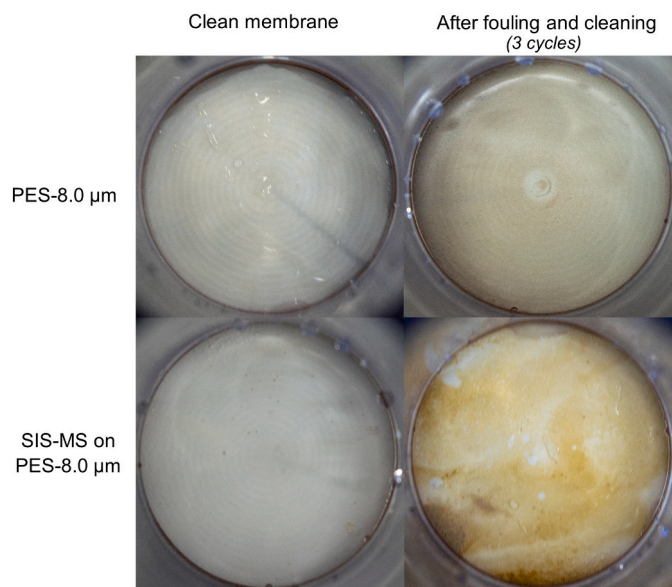


Fig. 14. Surface images of a commercial PES-8.0  $\mu\text{m}$  (top) and emerging SIS-MS on PES 8.0  $\mu\text{m}$  membrane (bottom). Clean membranes (left) and after fouling and cleaning (right).

improved rejection performances but still requires improvement in terms of fouling propensity and cleanability. Optical images to qualitatively illustrate and compare the fouling behavior of the emerging membrane against the commercial MF product are presented in Fig. 14.

The procedure will help optimize various innovative membrane materials currently under development by our team to identify the formulations that would demonstrate step change in performance in comparison to commercial products.

## 5. Conclusion

The study presented a bench-testing procedure developed for evaluating the performance of commercial and novel flat sheet MF/UF membranes for oil-water separation. The protocol mimics industrial conditions by using a representative synthetic PW solution and applying multiple consecutive oil-water separation with cleaning cycles. Several commercial MF/UF membranes having different pore size/MWCO and chemistry were acquired from multiple manufacturers and evaluated using the protocol in terms of water permeability, organics rejection, fouling, and cleanability. Selected observations from membrane performance evaluation which validated the protocol applicability include:

- For MF membranes with larger pore sizes, higher specific water flux and lower fouling tendency and organics rejection performance were achieved.
- For MF membranes with smaller pore sizes, lower specific water flux and higher fouling propensity were measured but with higher organics rejection.
- For UF membranes with larger MWCOs, higher specific water fluxes were observed, which were linearly correlated to increased membrane porosity.
- The fouling rate of UF membranes with different MWCOs was dependent on the fouling mechanism (e.g. cake filtration vs intermediate blocking) on the membrane surface.
- For membranes manufactured with the same polymer, variation in performance was found to be dependent on the difference of vendor membrane characterization, which was further supported by SEM analysis.

- For different membrane polymers acquired from the same vendor, PAN showed the lowest fouling tendency while PVDF showed the highest fouling propensity, which was also validated by FTIR.
- For different membrane polymers with the same MWCO from the same vendor, PAN had the lowest organics rejection while PVDF had the highest rejection.

Finally, the protocol steps were effectively applied on novel membrane materials under development to compare their performance against relevant commercial products. Hence, the robust bench-testing procedure is proposed to be utilized by researchers who are developing innovative membrane materials to allow for comparison of their new membranes against relevant commercial products for industrial applications.

## Funding information

Open Access funding provided by the Qatar National Library.

## Declaration of competing interest

The authors declare that they have no known competing financial interests or personal relationships that could have appeared to influence the work reported in this paper.

## Acknowledgments

The authors would like to acknowledge that this work was made possible through the support of Qatar National Research Fund (QNRF) as part of the Qatar National Priorities Research Program (NPRP) grant reference number of NPRP10-0127-170269. The content of this paper is solely the responsibility of the authors and does not necessarily represent the official views of ConocoPhillips or QNRF. The authors would also like to thank members from the ConocoPhillips Global Water Sustainability Center, Arnold Janson and Daren Dardor for their continuous support throughout this project. Special appreciation as well to our QNRF project partners from Qatar University, specifically Yara Elgawady and Ali El-Samak for their contribution to this project.

## References

- [1] Y. Peng, Z. Guo, Recent advances in biomimetic thin membranes applied in emulsified oil/water separation, *J. Mater. Chem. A* 4 (2016) 15749–15770, <https://doi.org/10.1039/C6TA06922C>.
- [2] A. Salahi, A. Gheshlaghi, T. Mohammadi, S.S. Madaeni, Experimental performance evaluation of polymeric membranes for treatment of an industrial oily wastewater, *Desalination* 262 (2010) 235–242, <https://doi.org/10.1016/j.desal.2010.06.021>.
- [3] Y. Yu, H. Chen, Y. Liu, V.S.J. Craig, C. Wang, L.H. Li, Y. Chen, Superhydrophobic and superoleophilic porous boron nitride nanosheet/polyvinylidene fluoride composite material for oil-polluted water cleanup, *Adv. Mater. Interfaces* 2 (2015), 1400267, <https://doi.org/10.1002/admi.201400267>.
- [4] S. Alzahrani, A.W. Mohammad, Challenges and trends in membrane technology implementation for produced water treatment: a review, *J. Water Process Eng.* 4 (2014) 107–133, <https://doi.org/10.1016/j.jwpe.2014.09.007>.
- [5] A. Fakhru'l-Razi, A. Pendashteh, L.C. Abdullah, D.R.A. Biak, S.S. Madaeni, Z. Z. Abidin, Review of technologies for oil and gas produced water treatment, *J. Hazard. Mater.* 170 (2009) 530–551, <https://doi.org/10.1016/j.jhazmat.2009.05.044>.
- [6] M. Seddighi, S.M. Hejazi, Water–oil separation performance of technical textiles used for marine pollution disasters, *Mar. Pollut. Bull.* 96 (2015) 286–293, <https://doi.org/10.1016/j.marpolbul.2015.05.011>.
- [7] J. Rubio, M.L. Souza, R.W. Smith, Overview of flotation as a wastewater treatment technique, *Miner. Eng.* 15 (2002) 139–155, [https://doi.org/10.1016/S0892-6875\(01\)00216-3](https://doi.org/10.1016/S0892-6875(01)00216-3).
- [8] S. Adham, A. Hussain, J. Minier-Matar, A. Janson, R. Sharma, Membrane applications and opportunities for water management in the oil & gas industry, *Desalination* (2018), <https://doi.org/10.1016/j.desal.2018.01.030>.
- [9] K. Farahbakhsh, S. Adham, D. Smith, Monitoring the integrity of low-pressure membranes, *J. Am. Water Works Assoc.* 95 (2003) 95–107, <https://doi.org/10.1002/j.1551-8833.2003.tb10390.x>.
- [10] T. Ahmad, C. Guria, A. Mandal, Synthesis, characterization and performance studies of mixed-matrix poly(vinyl chloride)-bentonite ultrafiltration membrane



- for the treatment of saline oily wastewater, *Process. Saf. Environ. Prot.* 116 (2018) 703–717, <https://doi.org/10.1016/j.psep.2018.03.033>.
- [11] J. Mueller, Y. Cen, R.H. Davis, Crossflow microfiltration of oily water, *J. Membr. Sci.* 129 (1997) 221–235, [https://doi.org/10.1016/S0376-7388\(96\)00344-4](https://doi.org/10.1016/S0376-7388(96)00344-4).
- [12] A. Salahi, M. Abbasi, T. Mohammadi, Permeate flux decline during UF of oily wastewater: experimental and modeling, *Desalination*. 251 (2010) 153–160, <https://doi.org/10.1016/j.desal.2009.08.006>.
- [13] S.N. Wan Ikhshan, N. Yusof, F. Aziz, N. Misdan, A.F. Ismail, W.J. Lau, J. Jaafar, W.N. Wan Salleh, N.H. Hayati Hairom, Efficient separation of oily wastewater using polyethersulfone mixed matrix membrane incorporated with halloysite nanotube-hydrated ferric oxide nanoparticle, *Sep. Purif. Technol.* 199 (2018) 161–169, <https://doi.org/10.1016/j.seppur.2018.01.028>.
- [14] R.M. Dorin, W.A. Phillip, H. Sai, J. Werner, M. Elimelech, U. Wiesner, Designing block copolymer architectures for targeted membrane performance, *Polymer* 55 (2014) 347–353, <https://doi.org/10.1016/j.polymer.2013.09.038>.
- [15] C. Li, Y. Ma, H. Li, G. Peng, A convenient method for the determination of molecular weight cut-off of ultrafiltration membranes, *Chin. J. Chem. Eng.* 25 (2017) 62–67, <https://doi.org/10.1016/j.cjche.2016.06.014>.
- [16] V. Hugo, T. Overview, *Introduction to Membrane Technology*, 2015, pp. 1–80, <https://doi.org/10.1016/B978-0-444-63362-0.00001-X>.
- [17] T. Rajasekhar, M. Trinadh, P. Veera Babu, A.V.S. Sainath, A.V.R. Reddy, Oil-water emulsion separation using ultrafiltration membranes based on novel blends of poly(vinylidene fluoride) and amphiphilic tri-block copolymer containing carboxylic acid functional group, *J. Membr. Sci.* 481 (2015) 82–93, <https://doi.org/10.1016/j.memsci.2015.01.030>.
- [18] Y. Elgawady, D. Ponnamma, S. Adham, M. Al-Maas, A. Ammar, K. Alamgir, M.A. A. Al-Maadeed, M.K. Hassan, Mesoporous silica filled smart super oleophilic fibers of triblock copolymer nanocomposites for oil absorption applications, *Emergent Mater.* 3 (2020) 279–290, <https://doi.org/10.1007/s42247-020-00111-3>.
- [19] S. Wang, J. Cai, W. Ding, Z. Xu, Z. Wang, Bio-inspired aquaporin containing double-skinned forward osmosis membrane synthesized through layer-by-layer assembly, *Membranes* (2017) 369–384, <https://doi.org/10.3390/membranes5030369>.
- [20] Y.P. Tang, S. Yuwen, T.S. Chung, M. Weber, C. Staudt, C. Maletzko, Synthesis of hyperbranched polymers towards efficient boron reclamation via a hybrid ultrafiltration process, *J. Membr. Sci.* 510 (2016) 112–121, <https://doi.org/10.1016/j.memsci.2016.03.024>.
- [21] X. Hu, Y. Yu, J. Zhou, Y. Wang, J. Liang, X. Zhang, Q. Chang, L. Song, The improved oil/water separation performance of graphene oxide modified Al<sub>2</sub>O<sub>3</sub> microfiltration membrane, *J. Membr. Sci.* 476 (2015) 200–204, <https://doi.org/10.1016/j.memsci.2014.11.043>.
- [22] P. Pi, K. Hou, C. Zhou, X. Wen, S. Xu, J. Cheng, S. Wang, A novel superhydrophilic- underwater superoleophobic Cu<sub>2</sub>S coated copper mesh for efficient oil-water separation, *Mater. Lett.* 182 (2016) 68–71, <https://doi.org/10.1016/j.matlet.2016.06.087>.
- [23] J.A. Prince, S. Bhuvana, V. Anbharasi, N. Ayyanar, K.V.K. Boodhoo, G. Singh, Ultra-wetting graphene-based PES ultrafiltration membrane – a novel approach for successful oil-water separation, *Water Res.* 103 (2016) 311–318, <https://doi.org/10.1016/j.watres.2016.07.042>.
- [24] M.T.M. Pendergast, R. Mika Dorin, W.A. Phillip, U. Wiesner, E.M.V. Hoek, Understanding the structure and performance of self-assembled triblock terpolymer membranes, *J. Membr. Sci.* 444 (2013) 461–468, <https://doi.org/10.1016/j.memsci.2013.04.074>.
- [25] H. Yang, Z. Wang, Q. Lan, Y. Wang, Antifouling ultrafiltration membranes by selective swelling of polystyrene/poly(ethylene oxide) block copolymers, *J. Membr. Sci.* 542 (2017) 226–232, <https://doi.org/10.1016/j.memsci.2017.08.015>.
- [26] D. Zhong, Z. Wang, Q. Lan, Y. Wang, Selective swelling of block copolymer ultrafiltration membranes for enhanced water permeability and fouling resistance, *J. Membr. Sci.* 558 (2018) 106–112, <https://doi.org/10.1016/j.memsci.2018.04.021>.
- [27] W. Chen, M. Wei, Y. Wang, Advanced ultrafiltration membranes by leveraging microphase separation in macrophase separation of amphiphilic polysulfone block copolymers, *J. Membr. Sci.* 525 (2017) 342–348, <https://doi.org/10.1016/j.memsci.2016.12.009>.
- [28] C. Cummins, R. Lundy, J.J. Walsh, V. Ponsinet, G. Fleury, M.A. Morris, Enabling future nanomanufacturing through block copolymer self-assembly: a review, *Nano Today* 35 (2020), 100936, <https://doi.org/10.1016/j.nantod.2020.100936>.
- [29] S. Qavi, A.P. Lindsay, M.A. Firestone, R. Foudazi, Ultrafiltration membranes from polymerization of self-assembled Pluronic block copolymer mesophases, *J. Membr. Sci.* 580 (2019) 125–133, <https://doi.org/10.1016/j.memsci.2019.02.060>.
- [30] Y. Luo, X. Wang, R. Zhang, M. Singh, A. Ammar, D. Cousins, M.K. Hassan, D. Ponnamma, S. Adham, M.A.A. Al-Maadeed, A. Karim, Vertically oriented nanoporous block copolymer membranes for oil/water separation and filtration, *Soft Matter* 16 (2020) 9648–9654, <https://doi.org/10.1039/d0sm00526f>.
- [31] D.A. Ladner, A. Subramani, M. Kumar, S.S. Adham, M.M. Clark, Bench-scale evaluation of seawater desalination by reverse osmosis, *Desalination*. 250 (2010) 490–499, <https://doi.org/10.1016/j.desal.2009.06.072>.
- [32] X. Shi, G. Tal, N.P. Hankins, V. Gitis, Fouling and cleaning of ultrafiltration membranes: a review, *J. Water Process Eng.* 1 (2014) 121–138, <https://doi.org/10.1016/j.jwpe.2014.04.003>.
- [33] P.H.H. Duong, T.S. Chung, S. Wei, L. Irish, Highly permeable double-skinned forward osmosis membranes for anti-fouling in the emulsified oil-water separation process, *Environ. Sci. Technol.* 48 (2014) 4537–4545, <https://doi.org/10.1021/es405644u>.
- [34] L. Luo, G. Han, T.S. Chung, M. Weber, C. Staudt, C. Maletzko, Oil/water separation via ultrafiltration by novel triangle-shape tri-bore hollow fiber membranes from sulfonated polyphenylenesulfone, *J. Membr. Sci.* 476 (2015) 162–170, <https://doi.org/10.1016/j.memsci.2014.11.035>.
- [35] X. Zhao, Y. Su, W. Chen, J. Peng, Z. Jiang, PH-responsive and fouling-release properties of PES ultrafiltration membranes modified by multi-functional block-like copolymers, *J. Membr. Sci.* 382 (2011) 222–230, <https://doi.org/10.1016/j.memsci.2011.08.014>.
- [36] S. Zhang, P. Wang, X. Fu, T.S. Chung, Sustainable water recovery from oily wastewater via forward osmosis-membrane distillation (FO-MD), *Water Res.* 52 (2014) 112–121, <https://doi.org/10.1016/j.watres.2013.12.044>.
- [37] G.S. Lai, M.H.M. Yusof, W.J. Lau, R.J. Gohari, D. Emadzadeh, A.F. Ismail, P.S. Goh, A.M. Isloor, M.R.D. Arzhandi, Novel mixed matrix membranes incorporated with dual-nanofillers for enhanced oil-water separation, *Sep. Purif. Technol.* 178 (2017) 113–121, <https://doi.org/10.1016/j.seppur.2017.01.033>.
- [38] G. Mustafa, K. Wynn, A. Buekenhoudt, V. Meynen, Antifouling grafting of ceramic membranes validated in a variety of challenging wastewaters, *Water Res.* 104 (2016) 242–253, <https://doi.org/10.1016/j.watres.2016.07.057>.
- [39] E.N. Tummons, J.W. Chew, A.G. Fane, V.V. Tarabara, Ultrafiltration of saline oil-in-water emulsions stabilized by an anionic surfactant: effect of surfactant concentration and divalent counterions, *J. Membr. Sci.* 537 (2017) 384–395, <https://doi.org/10.1016/j.memsci.2017.05.012>.
- [40] X. Zhu, A. Dudchenko, X. Gu, D. Jassby, Surfactant-stabilized oil separation from water using ultrafiltration and nanofiltration, *J. Membr. Sci.* 529 (2017) 159–169, <https://doi.org/10.1016/j.memsci.2017.02.004>.
- [41] H.S. Almarouf, M.S. Nasser, M.J. Al-Marri, M. Khraisheh, S.A. Onaizi, Demulsification of stable emulsions from produced water using a phase separator with inclined parallel arc coalescing plates, *J. Pet. Sci. Eng.* 135 (2015) 16–21, <https://doi.org/10.1016/j.petrol.2015.08.005>.
- [42] Y.M. Lin, G.C. Rutledge, Separation of oil-in-water emulsions stabilized by different types of surfactants using electrospun fiber membranes, *J. Membr. Sci.* 563 (2018) 247–258, <https://doi.org/10.1016/j.memsci.2018.05.063>.
- [43] H. Sun, Q. Wang, X. Li, X. He, Novel polyether-polyquaternium copolymer as an effective reverse demulsifier for O/W emulsions: demulsification performance and mechanism, *Fuel*. 263 (2020), <https://doi.org/10.1016/j.fuel.2019.116770>.
- [44] F.V. Adams, A. Peter, I.V. Joseph, O.P. Sylvester, A.F. Mulaba-Bafubandi, Purification of crude oil contaminated water using fly ash/clay, *J. Water Process Eng.* 30 (2019), 100471, <https://doi.org/10.1016/j.jwpe.2017.08.009>.
- [45] D. Dardor, M. Al-Maas, J. Minier-Matar, A. Janson, R. Sharma, M.K. Hassan, M. Al-Ali Al-Maadeed, S. Adham, Protocol for preparing synthetic solutions mimicking produced water from oil and gas operations, *ACS Omega* (2021), <https://doi.org/10.1021/acsomega.0c06065>.
- [46] A. Janson, A. Santos, M. Katebah, A. Hussain, J. Minier-matar, Assessing the biotreatability of produced water from a Qatari gas field, *SPE J.* (2014), <https://doi.org/10.1016/j.spe.2014.11.001>.
- [47] M. Cheryan, N. Rajagopalan, Membrane processing of oily streams. Wastewater treatment and waste reduction, *J. Membr. Sci.* 151 (1998) 13–28, [https://doi.org/10.1016/S0376-7388\(98\)00190-2](https://doi.org/10.1016/S0376-7388(98)00190-2).
- [48] H. Rabiee, M. Hossein, D. Abadi, V. Vatanpour, Preparation and characterization of emulsion poly(vinyl chloride) (EPVC)/TiO<sub>2</sub> nanocomposite ultrafiltration membrane, *J. Membr. Sci.* 472 (2014) 185–193, <https://doi.org/10.1016/j.memsci.2014.08.051>.
- [49] M. Matos, G. Gutiérrez, A. Lobo, J. Coca, C. Pazos, J.M. Benito, Surfactant effect on the ultrafiltration of oil-in-water emulsions using ceramic membranes, *J. Membr. Sci.* 520 (2016) 749–759, <https://doi.org/10.1016/j.memsci.2016.08.037>.
- [50] S. Zarghami, T. Mohammadi, M. Sadrzadeh, B. Van Der Brugge, Bio-inspired anchoring of amino-functionalized multi-wall carbon nanotubes (N-MWCNTs) onto PES membrane using polydopamine for oily wastewater treatment, *Sci. Total Environ.* 711 (2020), <https://doi.org/10.1016/j.scitotenv.2019.134951>.
- [51] G. Yi, S. Chen, X. Quan, G. Wei, X. Fan, H. Yu, Enhanced separation performance of carbon nanotube – polyvinyl alcohol composite membranes for emulsified oily wastewater treatment under electrical assistance, *Sep. Purif. Technol.* 197 (2018) 107–115, <https://doi.org/10.1016/j.seppur.2017.12.058>.
- [52] A. Rahimpour, S. Siavash, S. Ghorbani, A. Shokravi, The influence of sulfonated polyethersulfone (SPES) on surface nano-morphology and performance of polyethersulfone (PES) membrane, *Appl. Surf. Sci.* (2010), <https://doi.org/10.1016/j.apsusc.2009.10.014>.
- [53] Y.H. Chiao, S.T. Chen, M. Sivakumar, M.B.M.Y. Ang, T. Patra, J. Almodovar, S. R. Wickramasinghe, W.S. Hung, J.Y. Lai, Zwitterionic polymer brush grafted on polyvinylidene difluoride membrane promoting enhanced ultrafiltration performance with augmented antifouling property, *Polymers* 12 (2020) 1–12, <https://doi.org/10.3390/polym12061303>.
- [54] L. Jiang, Z. Tang, K.J. Park-Lee, D.W. Hess, V. Breedveld, Fabrication of non-fouling hydrophilic-oleophobic stainless steel mesh for oil-water separation, *Sep. Purif. Technol.* 184 (2017) 394–403, <https://doi.org/10.1016/j.seppur.2017.05.021>.